Macromolecules

Article

pubs.acs.org/Macromolecules

Contribution of Entanglements to Polymer Network Elasticity

F. Campise,[†] D. C. Agudelo,[‡] R. H. Acosta,[†] M. A. Villar,[‡] E. M. Vallés,[‡] G. A. Monti,*[,†] and D. A. Vega*[,§]

[†]IFEG−CONICET, FAMAF−Universidad Nacional de Córdoba, Córdoba, Argentina

[‡]Deparment of Chemical Engineering, Planta Piloto de Ingeniería Química, Universidad Nacional del Sur, CONICET, Bahía Blanca, Argentina

[§]Deparment of Physics, Instituto de Física del Sur (IFISUR), Universidad Nacional del Sur, CONICET, Bahía Blanca, Argentina

ABSTRACT: Trapped entanglements, cross-linker functionality, and elastically effective chains are the sources of elasticity of polymer networks and gels. However, despite more than 80 years of theoretical and experimental research in this field, still little is known about their relative contribution to network elasticity. In this work, we use double quantum nuclear magnetic resonance (DQ NMR) experiments to characterize the elasticity of model polymer networks prepared with cross-linkers of mixed functionality and control of structural defects. An order parameter that condensates the elastic response within the theoretical framework of the entangled phantom theory for rubber elasticity was identified. Standard lore dictates that low molecular weight precursors for the elastically active chains leads to a negligible contribution of trapped entanglements. Here we show that the contribution of trapped entanglements may equal the contribution coming from elastically active material and that it is independent of network topology.

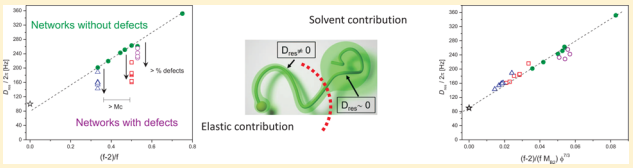

INTRODUCTION

The simplest models that capture the elastic behavior of polymer networks in terms of the average size of the polymer chains that make up the system (network strands) and the functionality of cross-linker points are the affine and phantom model.[1,2] In the affine model, cross-link junctions are fixed in space and move proportionally with the whole network. Thus, the deformation of each network strand is assumed to be the same as the macroscopic deformation imposed on the polymer network. In the phantom model, the cross-link junctions are not fixed in space but can fluctuate around their average positions.[3] As a consequence, the elasticity of the network is reduced by a factor $(f-2)/f$, with f being the functionality of the cross-linker. Since the phantom model is based on unrestricted fluctuations of ideal strands that are allowed to pass through each other, this theoretical frame provides a lower bound for the network elasticity. On the other hand, it has been observed that these models can underestimate the elasticity of real networks due to the contribution of trapped entanglements.[4] Defects, like entangled loops[5] and free and dangling molecules,[6] reduce the elasticity and dictate the nonrecoverable dissipative response, a key factor to design the relaxation dynamics for a wide variety of applications, including cosmetics, hydrogels, acoustic blankets, vibration suppression devices and shock absorbers (synthetic articular cartilage, automobile bumpers, helmets, etc.).

Departures from the classical rubber elasticity models[1,2] due to entanglements or defects are introduced in several models of rubber elasticity, like the "real elastic network theory"[5] or the constrained junction or slip-link models.[7−11]

In order to provide an insight on the structure−property relationships and to test the validity of the different theoretical models, a variety of experimental approaches, e.g., rheology,[4] disassembly spectrometry,[5,12] dielectric spectroscopy,[13] swelling,[14,15] neutron scattering, and ^1H multiple quantum NMR measurements,[16] have been employed. In particular, it has been shown that multiple quantum spectroscopy is a robust technique to characterize polymer structure and dynamics.[16−18]

It is based on the through space $^1H-^1H$ dipole−dipole coupling which is related to anisotropic segmental fluctuations of the monomeric units.[19]

In this work, double quantum (DQ) NMR experiments on model end-linked networks with cross-linkers of mixed functionality and well-known structural parameters were addressed to study the correlations between elasticity and network architecture. We study the relationship between the residual dipolar coupling constant D_{res} obtained by DQ experiments and the network topology on poly(dimethylsiloxane) (PDMS) networks with different average functionalities and accurately controlled contents of defects. Networks were obtained by end-linking monofunctional and difunctional telechelic prepolymers and a mixture of cross-linkers with different functionality (Figure 1a).

MATERIALS AND METHODS

Poly(dimethylsiloxane) (PDMS) model networks were obtained by hydrosilylation reaction between silane groups of different cross-linkers and end vinyl groups of prepolymers in the presence of a Pt salt as catalyst.[20] A commercial difunctional prepolymer, α,ω-divinylpoly(dimethylsiloxane) (B_2) (United Chemical Technologies, Inc.) was used to generate the elastic chains of the networks. Phenyltris(dimethylsiloxy)silane (A_3), tetrakis(dimethylsiloxy)silane (A_4)

Received: December 27, 2016
Revised: March 14, 2017
Published: March 23, 2017

DOI: 10.1021/acs.macromol.6b02784
Macromolecules 2017, 50, 2964−2972

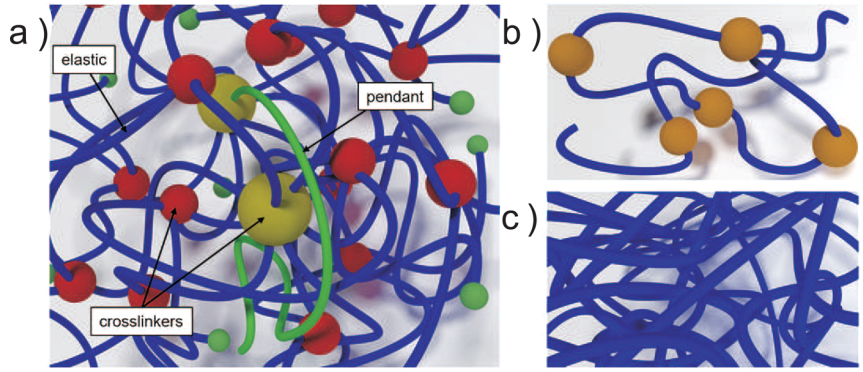

Figure 1. (a) Schematic representation of model silicone networks of mixed functionalities $f = 4$ and $f = 8$ obtained via the end-linking technique. The average cross-linker functionality can be prescribed through the relative ratio of cross-linkers. The content and size of the pendant chains can be independently controlled through the end-linking method. (b) In a reaction of $A_2 + B_2$ difunctional groups A_2 acts as chain extensors of the prepolymers B_2. (c) This reaction can lead to a network of entanglements that shows a transient elasticity.

Table 1. Networks with Variable Functionality (f), Extent of Reaction (r), Weight Fraction of Cross-Linkers with Variable Functionality (w_{A_4}; w_{A_8}), and Networks with Addition of Pendant Chains with Variable Weight Fractions (W_{B_1})[a]

network	cross-linker	r	w_{A_4} (wt %)	w_{A_8} (wt %)	f	W_{B_1} (wt %)	M_{nB_1} [g/mol]	M_c [g/mol]	M_C/M_{nB_2}	$D_{res}/2\pi$ [Hz]	$(1-\phi)_{TD}$	$(1-\phi)_{DQ}$	T [K]
0-F3-0	A_3	1.001	–	–	3	–	–	9460	1.19	202	0.07	0.07	303
0-F4-25	$A_3 + A_4$	1.002	0.254	–	3.25	–	–	8657	1.09	220	0.06	0.06	303
0-F4-60	$A_3 + A_4$	0.999	0.598	–	3.60	–	–	8590	1.09	243	0.05	0.05	303
0-F4-75	$A_3 + A_4$	0.999	0.745	–	3.76	–	–	8460	1.07	251	0.04	0.04	303
0-F4-100	A_4	1.000	1.000	–	4	–	–	8410	1.06	263	0.05	0.05	303
0-F8-100	A_8	1.000	–	1.000	8	–	–	8160	1.03	352	0.06	0.06	303
1-F8-25	$A_4 + A_8$	1.001	0.744	0.256	5	0.010	51300	8120	1.03	255	0.10	0.09	303
5-F8-25	$A_4 + A_8$	1.000	0.752	0.248	5	0.051	51300	8540	1.08	242	0.11	0.10	303
10-F8-25	$A_4 + A_8$	1.000	0.748	0.252	5	0.102	51300	8520	1.08	232	0.13	0.14	303
15-F8-25	$A_4 + A_8$	1.000	0.750	0.250	5	0.149	51300	8700	1.10	228	0.16	0.16	303

[a]The molecular weight for the difunctional precursors is M_n = 7900 g/mol. The molecular weight between cross-links M_c was calculated by the recursive method.[37−39] The fraction of relaxed pendant chains are determined both from CPMG experiments[6] ($(1-\phi)_{TD}$) and from DQ experiments[22] ($(1-\phi)_{DQ}$), showing a good agreement.

(United Chemical Technologies, Inc.), and octasilane POSS (Hybrid Plastics Inc.) (A_8) were used as cross-linkers in different proportions to produce "defect-free" networks with variable functionality (see the scheme of Figure 1). Here by "defect-free" networks we mean $A_f + B_2$ systems at the optimum conditions of reaction.

Systems with defects consistent of pendant chains were prepared by the addition of monofunctional ω-vinyl PDMS B_1 monodisperse prepolymers, synthesized by anionic polymerization of hexamethylcicletrisiloxane as reported elsewhere.[14,21] This networks were achieved by adding specific amounts of B_1 monofunctional chains to the reacting mixture of B_2 and the proper cross-linkers A_4 and A_8 in a stoichiometrically balanced system. The number-average molecular weight (M_{nB_2} = 7900 g/mol; M_{nB_1} = 51300 g/mol) and polydispersity ($(M_w/M_n)_{B_2}$ = 2.40; $(M_w/M_n)_{B_1}$ = 1.14) of the bi- and monofunctional precursors, B_2 and B_1, were determined through Size-Exclusion Chromatograpghy (SEC), using toluene as solvent. Further details regarding the characterization of the systems as well as the determination of molecular structure carried out by mean field theory can be found in the Appendix. Nomenclature and structural parameters are shown in Table 1 (Appendix). Details about the characterization of the systems with 20 wt % of monofunctional pendant chains with different molecular weight and functionalities f = 3 and f = 4 were studied in a previous work.[18] It is worthwhile noting that polymer networks prepared for this study have as small contents of undesired structural defects as possible. At the optimum reaction conditions it was found that the fraction of extracted material is below 3 wt % and as the reaction is carried out without diluents and B_2 precursors are large and flexible enough to have a nearly Gaussian end-to-end distance, the concentration of loops are negligible.[6] In addition, before NMR measurements, networks were subjected to soluble extraction for about one month using toluene as solvent. Thus, the only unavoidable defects in the structure are small contents of dangling chains resulting from the partial reaction of B_2 precursors.

For the determination of the residual dipolar coupling constant D_{res}, ^{1}H DQ−NMR experiments were performed in a Bruker minispec mq20 time-domain spectrometer, equipped with a permanent magnet that provides an operating magnetic field of 0.5 T, which corresponds to 19.9 MHz for protons. Typical values for the for the 90° pulses were 2.4 μs. Samples of roughly 4 mm high were centered on a 10 mm Wildman sample tube. Temperature was controlled with a Bruker BVT3000 temperature controller capable of maintaining a constant temperature within 0.1 °C. Experiments were carried out at 303 K for all samples, and repeated at 440 K for trifunctional networks with 20 wt % of monofunctional pendant material.

Transverse relaxation decay data were acquired using a compensated CPMG pulse sequence with a block of four alternated phases, $yy\bar{y}\bar{y}$, for the refocusing π pulses. In the analysis of the ^{1}H NMR experiments, the transverse magnetization decay can be described as the sum of a solid-like contribution, with relative weight ϕ, coming from elastically active chains and transiently trapped entanglements on the NMR time scale, in addition to a liquid-like contribution, with relative weight $1-\phi$, coming from the relaxed portions of the pendant chains. These values are obtained from the NMR signal time-based decay by a nonlinear least-squares fitting procedure.[6]

DOI: 10.1021/acs.macromol.6b02784
Macromolecules 2017, 50, 2964−2972

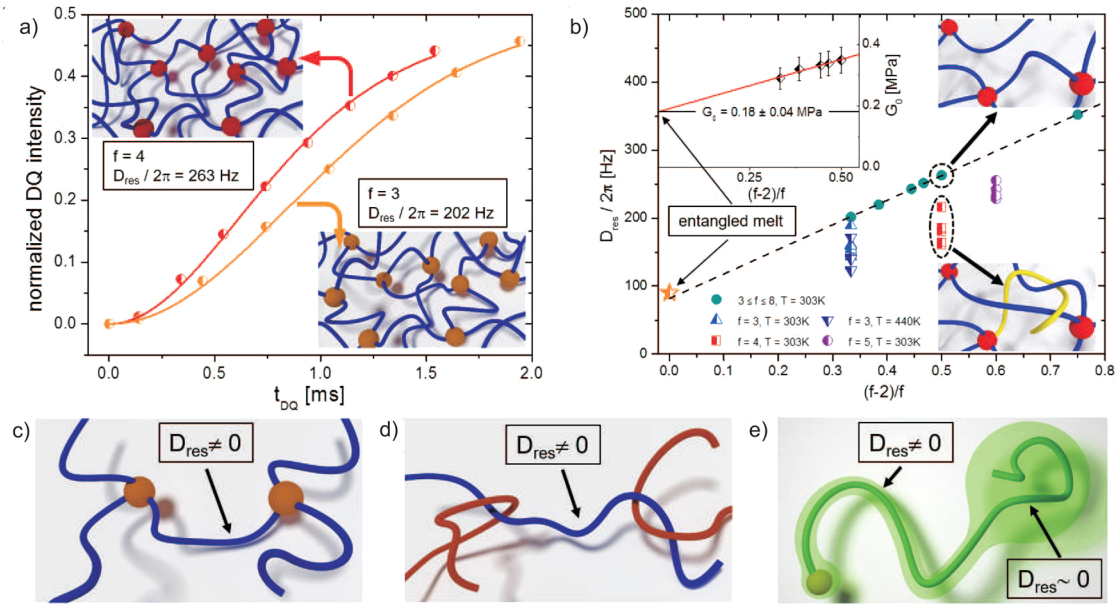

Figure 2. (a) Normalized DQ-NMR data for two representative networks; solid lines correspond to fittings with eq 1. (b) Residual dipolar coupling constant determined by NMR as a function of $(f-2)/f$. Networks with varying average functionality without defects (dots) follow a linear behavior (dashed line). Networks with different concentration of pendant chains are not well represented by the phantom model (half filled symbols). The open star symbol accounts for the $D_{res}/2\pi$ value for a well entangled melt of ≈140 kDa. Inset: Low frequency storage modulus G_0 as a function of $(f-2)/f$. Extrapolation to $f = 2$ leads to values of G_0 similar to those found in entangled melts. Panels c–e show the sources of D_{res} in polymer networks.

RESULTS AND DISCUSSION

Figure 2a shows the normalized intensity of the DQ signals as a function of the sequence pulse timing for tri- and tetra-functional polymer networks. ^{1}H DQ–NMR experiments were performed following the normalization procedure introduced by Saalwächter et al.[22] A signal dependent on the sequence pulse timing (τ_{DQ}) which is related to double quantum coherences is acquired. Further data analysis consists in a subtraction of a slow-decaying component related to the unentangled isotropically moving chain ends.[22] Residual dipolar couplings are obtained from the resulting data I_{nDQ} (see Figure 2a) by fitting the data to the equation:

$$I_{nDQ}(\tau_{DQ}) = \frac{1}{2}\left[1 - \frac{\exp\left(-\frac{\frac{2}{5}D_{res}^{\,2}\tau_{DQ}^{\,2}}{1+\frac{4}{5}\sigma^2\tau_{DQ}^{\,2}}\right)}{\sqrt{1+\frac{4}{5}\sigma^2\tau_{DQ}^{\,2}}}\right] \quad (1)$$

where σ represents the distribution in dipolar couplings.

According to the affine model, the elastic response of polymer networks is independent of the functionality of the cross-linking agent. However, D_{res}, a measure of the network elasticity, increases monotonously with f for "defect-free networks", in clear opposition with the predictions of the affine model. As shown in Figure 2b, D_{res} follows a linear dependence when plotted against $(f-2)/f$, in agreement with the predictions of the phantom model for the network elasticity. However, note also that D_{res} approaches a value different from zero when extrapolating the data toward $f = 2$, where the formation of a network is completely inhibited. An end-linking $A_2 + B_2$ reaction conducted with difunctional ($f = 2$) "cross-linkers", will not lead to a network but to linear chains with high molecular weight since A_2 groups act as chain extenders[23] that do not allow branching (Figure 1b). The fact that D_{res} approaches a value different from zero for $f = 2$ is a clear signature of the contribution of trapped entanglements to the network elasticity. The value of D_{res} obtained by extrapolation to $f = 2$ ($D_{res}/2\pi \sim 82$ *Hz*) agrees quite well with the experimental value reported by Vaca Chávez and Saalwächter for well entangled PDMS polymer melts. In this case, it was found that $D_{res}/2\pi \sim 90 \pm 10$ *Hz* for a polymer melt prepared with ≈140 kg/mol molecular weight chains,[24] similar to the molecular weight developed during the reaction of chain extension of p-bis(dimethylsilyl) benzene (A_2) and B_2 telechelic prepolymers.[23]

These results are in agreement with the data for the equilibrium shear modulus of the networks. The inset of Figure 2b shows the low frequency shear modulus G_0 as a function of $(f-2)/f$. Note that here the extrapolation to $f = 2$ leads to $G_0 \sim 0.18 \pm 0.2$ MPa, this value matches within error and the usual uncertainties the plateau modulus of entangled polymer melts ($G_0^{melt} \sim 0.2$ MPa), which is also a clear indication of the contribution of trapped entanglements to the network elasticity. Thus, both NMR data and elasticity indicate that these networks are well described by the phantom network for entangled strands. Within this approach and considering the contribution of trapped entanglements and the models by Lang and Sommer and Saalwächter et al.,[16,25–27] the residual dipolar coupling constant D_{res}^{df} for defect free networks can be expressed as

$$D_{res}^{df}/2\pi = \frac{A}{M_c}\frac{(f-2)}{f} + T_e D^o/2\pi \quad (2)$$

where M_c is the molecular weight between cross-links, $D^o/2\pi$ accounts for the residual dipolar coupling associated with a well entangled melt, T_e is the fraction of trapped entanglements and the proportionality factor A depends on the investigated polymer. Considering M_{B_2} as the molecular weight between

DOI: 10.1021/acs.macromol.6b02784
Macromolecules 2017, 50, 2964–2972

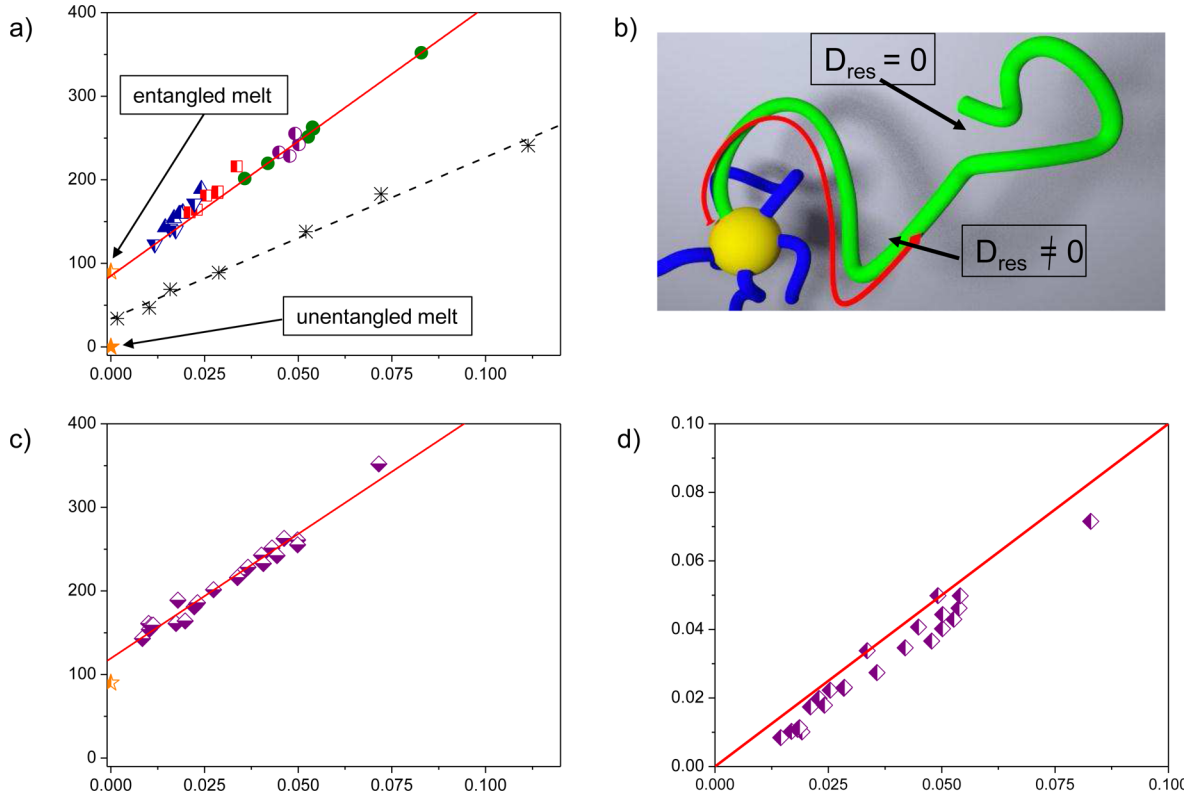

Figure 3. (a) D_{res} data vs experimental values for $\frac{f-2}{fM_{nB2}}\phi^{7/3}$ for different sets of polymer networks (symbols: see details in Figure 2; filled star symbol corresponds to low molecular weight PDMS melt (≈ 30 kDa)). This figure also includes the data by Chassé et al. for rPDMS (black asterisks).[16] Solid lines are linear fits through the data. Filled and half-filled star symbols corresponds to values of D_{res} for unentangled and entangled melts, respectively. (b) Schematic representation for the arm retraction mechanism for a pendant chain. Here s is the fractional distance along the primitive path where the free end have been retracted at time-scale τ_{NMR}. (c) D_{res} vs theoretical values for $\frac{f-2}{fM_c}\phi^{7/3}$. (d) Comparison between experimental and theoretical data for $\frac{f-2}{fM_c}\phi^{7/3}$. The continuous line is a linear fit through the data (slope 0.85 ± 0.02) and the dotted line have unity slope.

cross-links, by fitting the data in Figure 2b results in A = 2400 Hz kg/mol, different from the value predicted through a fixed-junction model and spin dynamics simulations for PDMS (A = 1266 Hz kg/mol).[28] Nonetheless, this difference may be explained by the fact that the latter has been derived on the basis of the affine model for tetrafunctional networks where $(f - 2)/f = 0.5$. Then the value A = 1266 Hz kg/mol may already contain the functionality dependence in its estimation, rendering a 'phantom derived' value A = 2532 Hz kg/mol which is certainly in good agreement with our fitted value A = 2400 Hz kg/mol, supporting our results. Values of T_e obtained here through NMR ($T_e = 0.91$) are in good agreement with the values obtained through rheology ($T_e = G_0/G_0^{melt} = 0.9$) and theoretical predictions ($T_e = 0.8$).[29] Thus, NMR experiments confirm that the sources of elasticity for these networks are the elastically active strands, cross-linkers and trapped entanglements (Figure 2c,d). Importantly, the linearity of D_{res} vs $(f - 2)/f$ clearly indicates that the fraction of trapped entanglements is independent of the topology of the network, which is expected to be controlled through the average functionality of the cross-linkers.

In Figure 2b, it is also clear that the phantom model does not completely describe the dipolar couplings obtained for networks with defects, where dipolar interactions are observed to diminish upon the presence of pendant polymer chains. Note that if the time scale of NMR exploration τ_{NMR}~ 1 ms overcomes the terminal relaxation time of the pendant chain, their contribution to the elasticity is negligible. Contrarily, for $\tau_{NMR} \lesssim \tau_e$, where τ_e is the Rouse time between entanglements, pendants contributes to D_{res} in a similar fashion as elastic strands.

Thus, as the relaxation of pendant chains is relatively slow, those chain segments transiently trapped within the network enhance the elasticity while the relaxed portion acts as an effective diluent for which $D_{res} = 0$ (Figure 2e). The contribution of the pendant chains to D_{res} must then be dependent on temperature. As temperature increases, terminal relaxation time of the pendant chains decreases and a smaller fraction of trapped entanglements contributes to D_{res}.

Previously, it has been shown that in the presence of a Θ solvent the plateau modulus G_0 of well entangled polymer melts scales as $G_0 \propto \phi^{7/3}$, where ϕ is the polymer concentration in the solution.[3,15] Following the arguments of Milner and McLeish for branched polymers[30−33] and considering the wide distribution of the relaxation spectrum of pendant chains, we can assume that the relaxed fraction $1 - \phi$ of pendant materials acts as an effective diluent to the network elasticity. This fraction can be obtained through time-domain NMR (TD-NMR) experiments.[6] In this case, the transverse magnetization decay can be described as the sum of a solid-like contribution, with relative weight ϕ, coming from elastically active chains and transient entanglements persisting on the NMR time scale, in addition to a liquid-like contribution, with relative weight $1 - \phi$, coming from the fraction of relaxed pendant material (see

DOI: 10.1021/acs.macromol.6b02784
Macromolecules 2017, 50, 2964−2972

the Appendix for more details). Figure 3a shows that, when plotted against $\frac{f-2}{fM_{nB2}}\phi^{7/3}$, D_{res} collapses the full set of data in a simple linear dependence, independently of the functionality, temperature of analysis, content of defect or molecular weight of pendant chains.

In order to test the validity of the $\phi^{7/3}$ scaling for another systems, in Figure 3a we also include the data by Chassé et al.,[16,34] for randomly cross-linked PDMS networks (rPDMS). For these networks, vinyl-functionalized polymers of relatively low molecular weight were cross-linked by using a bifunctional cross-linker. Although the values of M_c are model dependent,[34] within the concentration regime explored here the nearly linear dependence of D_{res} vs $\frac{f-2}{fM_c}\phi^{7/3}$ still holds, although network architecture of these polymers are completely different from the one studied here. Random cross-linking reaction leaves complex structures of loops and pendant chains of low molecular weight, which are relaxed at τ_{NMR}. Indeed, the size of defects and segments between branch points in this rPDMS are estimated to be below 5000 g/mol. Such defects would relax quickly ($t < 10^{-2}$ ms) on the time scale of τ_{NMR}. Note that extrapolation for the melt ($f\sim 2$) for this systems leads to $D^{\circ}/2\pi \sim 35$ Hz, above the value for an unentangled melt ($D_{res} = 0$) and well below the value corresponding to a linear entangled melt ($D_{res}/2\pi \sim 90$ Hz). However, as the random cross-linked structure contains a relatively large amount of unentangled branches, evidently in this case the network of trapped entanglements is very diluted.

From a theoretical perspective, the contribution of elastically active and pendant material to the transient elasticity can be described through the Miller−Macosko model for networks with mixed functionality combined with the relaxation dynamics of pendant chains. The addition of pendant chains affects the network architecture with a reduction in the density of elastically active chains (see Table 1). In general, the theoretical determination of the fraction of unrelaxed pendant material at a given time scale can be difficult, due to the complexity of the network and the architecture of the pendant chains. However, here pendant chains are linear, their content is well determined through the synthesis procedure and its relaxation proceeds via the arm retraction mechanism in a Pearson−Helfand potential.[33,35,36] According to this mechanism the rate of loss of conformational memory is entirely determined by the size of pendant chains, the molecular weight between entanglements and the Rouse time for an entangled strand;[18,30,32,33] in this case, the unrelaxed fraction of the pendant chains can be expressed as $\int \exp[-t/\tau(s)_{dangl}]\, ds$ where $\tau(s)_{dangl}$ is the temperature dependent retraction time[18] and s is the fractional distance back along the primitive path where the pendant chain free end has been retracted ($0 < s < 1$) (Figure 3b).

Figure 3c shows D_{res} as a function of the theoretical values for M_c and the temperature dependent fraction $\phi(t = \tau_{NMR} = 1$ ms,$T)$ that contribute to the solid-like behavior of the NMR response. Similarly to the experimental data shown in Figure 3a, theoretical values for $\frac{f-2}{fM_c}\phi^{7/3}$ also shows a linear dependence with D_{res}. However, note in Figure 3d that although theoretical and experimental results for $\frac{f-2}{fM_c}\phi^{7/3}$ are linearly correlated, M_{B_2} underestimates M_c by about a 15% due to the defects that reduces the density of elastically active cross-linkers.

CONCLUSIONS

The good agreement between theory and experimental data suggests that NMR can provide a fast and highly effective microscopic technique to test different theories for network elasticity and to quantify the key network parameters that control both, elastic and dissipative properties. We expect that this technique will find application in addressing a variety of questions ranging from fundamental materials science to applied discovery in the field of polymer networks and gels. In addition, the ability of NMR to estimate the network architecture should enable scientists to establish new synthetic routes to control the formation of complex topologies, and thereby optimize the response function of these materials.

APPENDIX

Networks of Mixed Functionalities

Model PDMS networks were obtained by the hydrosylilation reaction, based on the addition of hydrogen silanes from cross-linker molecules of different functionalities to the end vinyl groups present in the prepolymer molecules.

The chemical structure of the octasilane (POSS) employed as octa-funtional cross-linker ($f = 8$) is shown in Figure 4. The details abouth the chemical structure of the tri- and tetra-functional cross-linkers were reported elsewhere.[14]

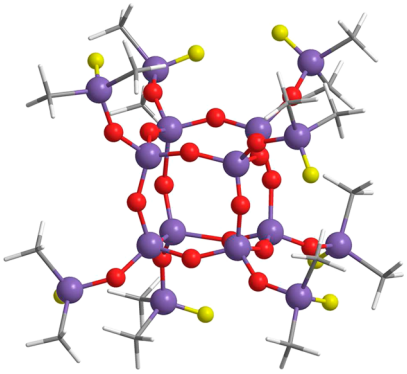

Figure 4. Schematic representation of the chemical structure of the octasilane cross-linker agent.

Tables 1 and 2 show the main structural parameters associated with the different polymer networks employed here.

Statistical Properties of the Polymer Networks

The presence of defects within the network reduces its elasticity and also affects its dynamic response. Since we deal with extracted samples without soluble material, the dominant defects are linear dangling chains. As these chains are entangled and its dynamic of relaxation is quite slow, there is a fraction near the free end of this material that behaves as a dynamic solvent to the rest of the network. In order to quantify theoretically the relaxed fraction of pendants, it is necessary to know their content and also their relaxational dynamics.

Here we first analyse the equilibrium structure of the different networks through a modified version of the Miller−Macosko model.[38,39] Then, the contribution of the transient entanglements to D_{res} is described through the arm retraction process in a Pearson−Helfand potential, as the classical reptation observed in linear polymer melts is completely inhibited.

DOI: 10.1021/acs.macromol.6b02784
Macromolecules 2017, 50, 2964−2972

Table 2. Tri- and Tetrafunctional Polymer Networks Prepared with B_2 Chains with M_n = 10800 g/mol and 20 wt % of Linear Pendant Chains of Different Molecular Weights

network	cross-linker	r	f	W_{B_1} (wt %)	M_{nB_1} [g/mol]	M_c [g/mol]	M_C/M_{nB_2}	$D_{res}/2\pi$ [Hz]	$(1-\phi)_{TD}$	$(1-\phi)_{DQ}$	T [K]
0-F3	A_3	1.02	3	–	–	14500	1.34	189	0.10	*a*	303
20-F3-B1	A_3	1.01	3	0.202	26700	19500	1.8	143	0.28	*a*	303
20-F3-B2	A_3	1.01	3	0.201	51800	18000	1.66	154	0.23	*a*	303
20-F3-B3	A_3	1.05	3	0.199	62100	18700	1.73	161	0.23	*a*	303
20-F3-B4	A_3	1.04	3	0.201	92300	17800	1.65	159	0.20	*a*	303
20-F3-B5	A_3	1.02	3	0.199	125000	18200	1.68	159	0.19	*a*	303
0-F3	A_3	1.01	3	0.202	26700	19500	1.8	171.7	0.13	0.19	440
20-F3-B1	A_3	1.01	3	0.201	51800	18000	1.66	122.9	0.34	0.38	440
20-F3-B2	A_3	1.05	3	0.199	62100	18700	1.73	141.7	0.25	0.23	440
20-F3-B3	A_3	1.04	3	0.201	92300	17800	1.65	139.6	0.22	0.29	440
0-F4	A_4	1.03	4	–	–	11500	1.06	216	0.13	*a*	303
20-F4-B1	A_4	1.03	4	0.217	26700	13600	1.26	161	0.29	*a*	303
20-F4-B2	A_4	1.01	4	0.203	51800	13600	1.26	164	0.26	*a*	303
20-F4-B3	A_4	1.02	4	0.209	62100	12900	1.19	181	0.23	*a*	303
20-F4-B4	A_4	1.04	4	0.214	92300	12500	1.16	184	0.19	*a*	303
20-F4-B5	A_4	1.00	4	0.221	125000	12500	1.16	186	0.19	*a*	303

[a]Data extracted from ref 18, where a DQ filter was implemented to remove the contribution from relaxed pendant material.

$A_f + A_k + B_2$ System

The networks employed in this study are prepared by reacting a mixture of a bifunctional prepolymer with reactive functional groups at the chain ends (B_2) and mixtures of polyfunctional cross-linkers A_f and A_k (f = 3,4; k = 3,8). The structure of the polymer network obtained by this procedure depends on the maximum extent of reaction (p) and the relative contents in which the precursors are mixed in the initial formulation of the cross-linking reaction.

To model the network structure we consider the approximations of the Miller–Macosko model:[37−39] (a) all functional groups of the same type are equally reactive, (b) all groups react independently of one another, and (c) the fraction of closed loops is negligibly small.

According to this approach, once the fraction of solubles have been experimentally determined, the model equations can be employed to determine the maximum extent of reaction and then the fractions of elastic and pendant material.

For the system $A_f + A_k + B_2$, the initial stoichiometric imbalance is given by

$$r = \frac{f[A_f]_0 + k[A_k]_0}{2[B_2]_0} \tag{3}$$

where $[A_f]_0$, $[A_k]_0$, and $[B_2]_0$ are the initial concentrations of cross-linkers and difunctional reacting groups, respectively. The relative concentration of f groups w can be expressed as

$$w = \frac{f[A_f]_0}{f[A_f]_0 + k[A_k]_0} \tag{4}$$

The weight fraction of cross-linkers A_f (W_{A_f}) and A_k (W_{A_k}) and difunctional prepolymers B_2 (W_{B_2}) are given by

$$W_{A_f} = \frac{M_{nA_f}}{M_{nA_f} + \frac{f}{2wr}M_{nB_2} + \frac{f}{k}\frac{(1-w)}{w}M_{nA_k}} \tag{5}$$

$$W_{A_k} = \frac{M_{nA_k}}{M_{nA_k} + \frac{k}{2(1-w)r}M_{nB_2} + \frac{k}{f}\frac{w}{(1-w)}M_{nA_f}} \tag{6}$$

$$W_{B_2} = \frac{M_{nB_2}}{M_{nB2} + \frac{2wr}{f}M_{nA_f} + \frac{2(1-w)r}{k}M_{nA_k}} \tag{7}$$

where M_{nA_f}, M_{nA_k}, and M_{nB_2} are the molecular weights of the cross-linkers A_f, A_k and difunctional chains B_2, respectively.

On the basis of the Miller–Macosko model, we define $P(F^{out}_{A,B})$ ($P(F^{in}_{A,B})$) as the probability that, looking out (in) from an A or B group, the reaction leads to a finite or dangling structure rather than to the infinite network.[39] Following the recursive approach, we have[38]

$$P(F^{in}_A) = wP(F^{out}_A)^{f-1} + (1-w)P(F^{out}_A)^{k-1} \tag{8}$$

$$P(F^{out}_A) = (1-p) + pP(F^{in}_B) \tag{9}$$

$$P(F^{in}_B) = P(F^{out}_B) \tag{10}$$

$$P(F^{out}_B) = (1-rp) + rpP(F^{in}_A) \tag{11}$$

$$P(F^{out}_B) = (1-rp^2) + rp^2wP(F^{out}_A)^{f-1} + rp^2(1-w)P(F^{out}_A)^{k-1} \tag{12}$$

In terms of these probabilities, the weight fraction of elastic W_E, pendant W_P, and soluble material W_S, can be expressed as

$$W_E = W_{A_f}\left[(1-P(F^{out}_A)^f) + \sum_{i=2}^{f-1}\binom{f}{i}\left(\frac{i}{f}\right)[P(F^{out}_A)]^{f-i}[1-P(F^{out}_A)]^i\right] + W_{A_k}\left[(1-P(F^{out}_A)^k) + \sum_{i=2}^{k-1}\binom{k}{i}\left(\frac{i}{k}\right)[P(F^{out}_A)]^{k-i}[1-P(F^{out}_A)]^i\right] + W_{B_2}(1-P(F^{out}_B)^2) \tag{13}$$

DOI: 10.1021/acs.macromol.6b02784
Macromolecules 2017, 50, 2964−2972

$$W_P = W_{A_f}\left[fP(F_A^{out})^{f-1}(1 - P(F_A^{out})) + \sum_{i=2}^{f-1}\binom{f}{i}\left(\frac{f-i}{f}\right)[P(F_A^{out})]^{f-i}[1 - P(F_A^{out})]^i\right] + W_{A_k}\left[kP(F_A^{out})^{k-1}(1 - P(F_A^{out})) + \sum_{i=2}^{k-1}\binom{k}{i}\left(\frac{k-i}{k}\right)[P(F_A^{out})]^{k-i}[1 - P(F_A^{out})]^i\right] + 2W_{B_2}P(F_B^{out})(1 - P(F_B^{out})) \quad (14)$$

$$W_S = W_{A_f}P(F_B^{out})^f + W_{A_k}P(F_B^{out})^k + W_{B_2}P(F_B^{out})^2 \quad (15)$$

$A_f + A_k + B_2 + B_1$ System

In this case, the relative content v of B_2 reactive groups and the stoichiometric imbalance r are given by

$$v = \frac{2[B_2]_0}{2[B_2]_0 + [B_1]_0} \quad (16)$$

$$r = \frac{f[A_f]_0 + k[A_k]_0}{2[B_2]_0 + [B_1]_0} \quad (17)$$

The weight fraction of cross-linkers A_f (W_{A_f}) and A_k (W_{A_k}), difunctional prepolymers B_2 (W_{B_2}) and monofunctional prepolymers B_1 (W_{B_1}) can be expressed as

$$W_{A_f} = \frac{M_{nA_f}}{M_{nA_f} + \frac{fv}{2wr}M_{nB_2} + \frac{f}{k}\frac{(1-w)}{w}M_{nA_k} + \frac{f(1-v)}{wr}M_{nB_1}} \quad (18)$$

$$W_{A_k} = \frac{M_{nA_k}}{M_{nA_k} + \frac{kv}{2(1-w)r}M_{nB_2} + \frac{k}{f}\frac{w}{(1-w)}M_{nA_f} + \frac{k(1-v)}{(1-w)r}M_{nB_1}} \quad (19)$$

$$W_{B_2} = \frac{M_{nB_2}}{M_{nB_2} + \frac{2wr}{fv}M_{nA_f} + \frac{2(1-w)r}{kv}M_{nA_k} + \frac{2(1-v)}{v}M_{nB_1}} \quad (20)$$

$$W_{B_1} = \frac{M_{nB_1}}{M_{nB_1} + \frac{2wr}{f(1-v)}M_{nA_f} + \frac{2(1-w)r}{k(1-v)}M_{nA_k} + \frac{v}{2(1-v)}M_{nB_2}} \quad (21)$$

For this system, the probabilities become

$$P(F_A^{in}) = wP(F_A^{out})^{f-1} + (1-w)P(F_A^{out})^{k-1} \quad (22)$$

$$P(F_A^{out}) = (1-p) + pP(F_B^{in}) \quad (23)$$

$$P(F_B^{in}) = vP(F_B^{out}) \quad (24)$$

$$P(F_B^{out}) = (1-rp) + rpP(F_A^{in}) \quad (25)$$

$$P(F_B^{out}) = (1 - rp^2v) + rp^2vwP(F_A^{out})^{f-1} + rp^2v(1-w)P(F_A^{out})^{k-1} \quad (26)$$

In terms of these probabilities, the weight fractions of elastic W_E, pendant W_P, and soluble material, are

$$W_E = W_{A_f}\left[(1 - P(F_A^{out})^f) + \sum_{i=2}^{f-1}\binom{f}{i}\left(\frac{i}{f}\right)[P(F_A^{out})]^{f-i}[1 - P(F_A^{out})]^i\right] + W_{A_k}\left[(1 - P(F_A^{out})^k) + \sum_{i=2}^{k-1}\binom{k}{i}\left(\frac{i}{k}\right)[P(F_A^{out})]^{k-i}[1 - P(F_A^{out})]^i\right] + W_{B_2}(1 - P(F_B^{out})^2) \quad (27)$$

$$W_P = W_{A_f}\left[fP(F_A^{out})^{f-1}(1 - P(F_A^{out})) + \sum_{i=2}^{f-1}\binom{f}{i}\left(\frac{f-i}{f}\right)[P(F_A^{out})]^{f-i}[1 - P(F_A^{out})]^i\right] + W_{A_k}\left[kP(F_A^{out})^{k-1}(1 - P(F_A^{out})) + \sum_{i=2}^{k-1}\binom{k}{i}\left(\frac{k-i}{k}\right)[P(F_A^{out})]^{k-i}[1 - P(F_A^{out})]^i\right] + 2W_{B_2}P(F_B^{out})(1 - P(F_B^{out})) + W_{B_1}(1 - P(F_B^{out})) \quad (28)$$

$$W_S = W_{A_f}P(F_B^{out})^f + W_{A_k}P(F_B^{out})^k + W_{B_2}P(F_B^{out})^2 + W_{B_1}P(F_B^{out}) \quad (29)$$

Molecular Weight between Entanglements M_C

For both systems described above, the molecular weight between cross-linker points can be expressed as

$$M_C = W_E/\nu \quad (30)$$

where the fraction of elastically effective network chains ν is given by

$$\nu = W_{A_f}/M_{A_f}\left[\sum_{i=3}^{f-1}\binom{f}{i}\left(\frac{i}{2}\right)[P(F_A^{out})]^{f-i}[1 - P(F_A^{out})]^i\right] + W_{A_k}/M_{A_k}\left[(\sum_{i=3}^{k-1}\binom{k}{i}\left(\frac{i}{2}\right)[P(F_A^{out})]^{k-i}[1 - P(F_A^{out})]^i\right] \quad (31)$$

Tables 1 and 2 shows the values of M_C calculated with this model and the ratio between M_C and the molecular weight between cross-linkers M_{nB_2}.

While the previous approach allows to estimate the total fraction of pendants, at the time-scale associated with the NMR measurements these chains are not completely relaxed and thus contributes partially to the network elasticity (Fig. 5). Thus, in order to know the fraction of pendants that enhances the solid-like NMR signal it is necessary to model its transient contribution to the network elasticity. In the next section, we employ the tube model and the arm retraction concept to calculate the fraction of pendants that contributes as elastic material to the NMR signal.

DOI: 10.1021/acs.macromol.6b02784
Macromolecules 2017, 50, 2964−2972

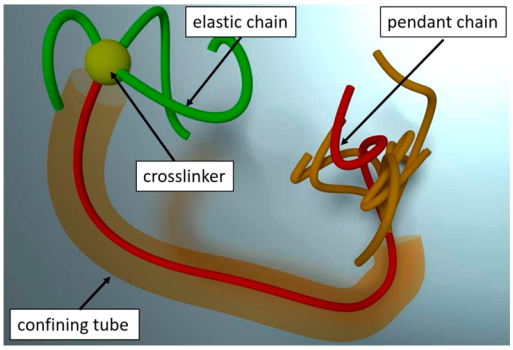

Figure 5. Schematic representation for the arm retraction mechanism for a pendant chain. The pendant chain is confined within an effective tube made of the elastically active chains. As one of the chain ends is linked to the network, it can only fluctuate around the equilibrium position of the cross-linker (yellow sphere). The pendant loose the memory of its initial configuration by retracting the free end along its confining tube and re-emerging along a different path. At the time scale of NMR exploration, the relaxed fraction of the pendant can not contribute to D_{res}.

Arm Retraction

The fraction of unrelaxed pendant material at the time scale of NMR experiments can be determined through the model of Doi and Kuzuu[35] and Pearson and Helfand[36] for the dynamics of branched polymers trapped in a fixed network of obstacles. According to this model, the fraction of tube surviving from the initial configuration $\chi(t)$, can be expressed as[31]

$$\chi(t) = \int \exp[-t/\tau(s)]\, ds \tag{32}$$

where $\tau(s)$ is the characteristic retraction time and s is the fractional distance back along the primitive path where the pendant chain free end has been retracted ($0 < s < 1$) (see also Figure 3b). The relaxation time $\tau(s)$ depends only on the effective number of entanglements in which the pendant chain is involved and the Rouse time between entanglements τ_e. At short times the chain moves under the action of many Rouse modes and the fast relaxation process is dominated by a one-dimensional Rouse-like dynamic characterized by $\tau_f(s)$

$$\tau_f(s) = \frac{225\pi^3}{256}\tau_e n_e^4 s^4 \tag{33}$$

where n_e is the number of entanglements. $\tau_f(s)$ controls the lack of configurational memory at short times, up to time-scales such that $s = s_d$ of order $s_d \sim \sqrt{\frac{1}{n_e}}$. Beyond s_d, retraction becomes increasingly slow and the relaxation process at time-scales $\tau_s(s)$ is controlled by the "arm retraction" mechanism, where

$$\tau_s(s, n_e) = -\frac{1}{2} I\pi^3 n_e^2 \tau_e \operatorname{erf}\left[I\sqrt{\frac{15n_e}{8}}\, s\right] \tag{34}$$

where $I = \sqrt{-1}$ and $\operatorname{erf}[x]$ is the error function.

In this case, the crossover between $\tau_f(s)$ and $\tau_s(s)$ can be determined through the crossover formulas:[30]

$$\tau_{pend}(s, n_e) = \frac{\tau_f(s, n_e)\tau_s(s, n_e)\exp U_{PH}(s)}{\tau_s(s, n_e) + \tau_s(s, n_e)\exp U_{PH}(s)} \tag{35}$$

Here $U_{PH}(s)$ is the Pearson-Helfand potential $U_{PH}(s) = 15/8\, n_e s^2$.

Taking into account the molecular weight distribution of the pendant material, the fraction of unrelaxed material at time $t = \tau_{NMR} \sim 1\ ms$ can be determined as $\chi = \int_0^\infty dn_e \times \int_0^1 ds\ P(n_e) \exp[-\tau_{NMR}/\tau(s,n_e)]$. Here $P(n_e)$ is the relative volume fraction of defects with average number of entanglements n_e. $P(n_e)$ can be determined through the molecular weight distribution of B_1 and B_2 chains and the mean field description of the network structure ($\int_0^\infty dn_e\ P(n_e) = 1$).[33]

Given that in our system the maximum extent of reaction reaches a relatively high value ($p \sim 1$), polymer networks always present controllable contents of pendant material. In the system $A_f + A_k + B_2$ these pendant material is mainly constituted by partially reacted linear B_2 chains that are attached to the network only through one chain end. In addition to the B_2 pendants, the system $A_f + A_k + B_2 + B_1$ also contains ad-hoc contents of linear B_1 pendants. As the molecular weight of the B_2 and B_1 pendants is different, there are different fractions χ_1 and χ_2 contributing to D_{res}. Here, χ_1 and χ_2 are the fractions of unrelaxed pendant material arising from B_1 monofunctional chains, and partially reacted B_2 chains, respectively.[18] Then, the concentration ϕ of polymer that remains unrelaxed at τ_{NMR} is $\phi = 1 - (1 - \chi_1)W_{B_1} - (1 - \chi_2)W_{B_2}$, where W_{B_1} is the weight fraction of monofunctional B_1 chains added to the network, and W_{B_2} accounts for the weight fraction of partially reacted bifunctional B_2 chains.

D_{res} Data from Networks Investigated by Chaseé et al

In Figure 3, we have included the experimental NMR data from Chassé et al.[16,34] In this case, the randomly cross-linked networks were obtained through vinyl-functionalized polymers of relatively low molecular weight cross-linked by using a 2-functional cross-linker. In order to compare these data with our results, we have employed the values of M_c determined through eqs 1 and 6 in ref 34 and the polymer concentration of defects ($\phi = 1 - w_{def}$) and D_{res} values reported in ref 16.

AUTHOR INFORMATION

Corresponding Authors

*(G.A.M.) E-mail: monti@famaf.unc.edu.ar.
*(D.A.V.) E-mail: dvega@uns.edu.ar.

Notes

The authors declare no competing financial interest.

ACKNOWLEDGMENTS

We express our gratitude to the Universidad Nacional del Sur, to Research Councils of Argentina: CONICET, ANPCyT PICT 2014-1295 and SeCyT-UNC which supported this work.

REFERENCES

(1) Wall, F. T.; Flory, P. J. Statistical thermodynamics of rubber elasticity. *J. Chem. Phys.* **1951**, *19* (12), 1435−1439.
(2) James, H. M.; Guth, E. Theory of the elastic properties of rubber. *J. Chem. Phys.* **1943**, *11* (10), 455−481.
(3) Rubinstein, M., Colby, R. H. *Polymer Physics (Chemistry)*; Oxford University Press: 2003.
(4) Gottlieb, M.; Macosko, C. W.; Benjamin, G. S.; Meyers, K. O.; Merrill, E. W. Equilibrium modulus of model poly(dimethylsiloxane) networks. *Macromolecules* **1981**, *14* (4), 1039−1046.
(5) Zhong, M.; Wang, R.; Kawamoto, K.; Olsen, B. D.; Johnson, J. A. Quantifying the impact of molecular defects on polymer network elasticity. *Science* **2016**, *353* (6305), 1264−1268.
(6) Campise, F.; Roth, L. E.; Acosta, R. H.; Villar, M. A.; Vallés, E. M.; Monti, G. A.; Vega, D. A. Contribution of linear guest and structural pendant chains to relaxational dynamics in model polymer

DOI: 10.1021/acs.macromol.6b02784
Macromolecules 2017, 50, 2964−2972

networks probed by time-domain 1h nmr. *Macromolecules* **2016**, *49*, 387−394.
(7) Ball, R. C.; Doi, M.; Edwards, S. F.; Warner, M. Elasticity of entangled networks. *Polymer* **1981**, *22*, 1010−1016.
(8) Edwards, S. F.; Vilgis, T. A. The tube model theory of rubber elasticity. *Rep. Prog. Phys.* **1988**, *51*, 243−297.
(9) Erman, B.; Mark, J. E. Rubber-Like Elasticity. *Annu. Rev. Phys. Chem.* **1989**, *40*, 351−374.
(10) Heinrich, G.; Straube, E.; Helmis, E. Rubber elasticity of polymer networks: Theories. *Adv. Polym. Sci.* **1988**, *85*, 33−87.
(11) Vilgis, T. A.; Erman, B. Comparison of the Constrained Junction and the Slip-Link Models of Rubber Elasticity. *Macromolecules* **1993**, *26*, 6657−6659.
(12) Wang, R.; Alexander-Katz, A.; Johnson, J. A.; Olsen, B. D. Universal cyclic topology in polymer networks. *Phys. Rev. Lett.* **2016**, *116*, 188302.
(13) Nicolai, T.; Prochazka, F.; Durand, D. Comparison of polymer dynamics between entanglements and covalent cross-links. *Phys. Rev. Lett.* **1999**, *82*, 863−866.
(14) Villar, M. A.; Vallés, E. M. Influence of pendant chains on mechanical properties of model poly(dimethylsiloxane) networks. 2. viscoelastic properties. *Macromolecules* **1996**, *29* (11), 4081−4089.
(15) Roth, L. E.; Agudelo, D. C.; Ressia, J. A.; Gómez, L. R.; Vallés, E. M.; Villar, M. A.; Vega, D. A. Viscoelastic response of linear defects trapped in polymer networks. *Eur. Polym. J.* **2015**, *64*, 1−9.
(16) Chassé, W.; Lang, M.; Sommer, J.-U.; Saalwächter, K. Cross-Link Density Estimation of Pdms Networks with Precise Consideration of Networks Defects. *Macromolecules* **2012**, *45* (2), 899−912.
(17) Chassé, W.; Saalwächter, K.; Sommer, J.-U. Thermodynamics of swollen networksas reflected in segmental orientation correlations. *Macromolecules* **2012**, *45* (13), 5513−5523.
(18) Acosta, R. H.; Monti, G. A.; Villar, M. A.; Vallés, E. M.; Vega, D. A. Transiently trapped entanglements in model polymer networks. *Macromolecules* **2009**, *42* (13), 4674−4680.
(19) Baum, J.; Pines, A. Nmr studies of clustering in solids. *J. Am. Chem. Soc.* **1986**, *108* (24), 7447−7454.
(20) Vallés, E. M.; Macosko, C. W. Properties of networks formed by end linking of poly(dimethylsiloxane). *Macromolecules* **1979**, *12* (4), 673−679.
(21) Vega, D. A.; Villar, M. A.; Vallés, E. M.; Steren, C. A.; Monti, G. A. Comparison of mean-field theory and1h nmr transversal relaxation of poly(dimethylsiloxane) networks. *Macromolecules* **2001**, *34* (2), 283−288.
(22) Saalwächter, K.; Ziegler, P.; Spyckerelle, O.; Haidar, B.; Vidal, A.; Sommer, J.-U. 1h multiple-quantum nuclear magnetic resonance investigations of molecular order distributions in poly(dimethylsiloxane) networks: Evidence for a linear mixing law in bimodal systems. *J. Chem. Phys.* **2003**, *119* (6), 3468−3482.
(23) Roth, L. E.; Vallés, E. M.; Villar, M. A. Bulk hydrosilylation reaction of poly(dimethylsiloxane) chains catalyzed by a platinum salt: Effect of the initial concentration of reactive groups on the final extent of reaction. *J. Polym. Sci., Part A: Polym. Chem.* **2003**, *41* (8), 1099−1106.
(24) Vaca Chávez, F.; Saalwächter, K. Time-domain NMR observation of entangled polymer dynamics: Analytical theory of signal functions. *Macromolecules* **2011**, *44* (6), 1560−1569.
(25) Saalwächter, K.; Herrero, B.; López-Manchado, M. A. Chemical shift-related artifacts in nmr determinations of proton residual dipolar couplings in elastomers. *Macromolecules* **2005**, *38* (9), 4040−4042.
(26) Lang, M.; Sommer, J.-U. Analysis of entanglement length and segmental order parameter in polymer networks. *Phys. Rev. Lett.* **2010**, *104*, 177801 DOI: 10.1103/PhysRevLett.104.177801.
(27) Syed, I. H.; Stratmann, P.; Hempel, G.; Klüppel, M.; Saalwächter, K. Entanglements, Defects, and Inhomogeneities in Nitrile Butadiene Rubbers: Macroscopic versus Microscopic Properties. *Macromolecules* **2016**, *49* (23), 9004−9016.
(28) Saalwächter, K.; Herrero, B.; López-Manchado, M. A. Chain order and cross-link density of elastomers as investigated by proton multiple-quantum nmr. *Macromolecules* **2005**, *38*, 9650−9666.
(29) Tsenoglou, C. Rubber elasticity of cross-linked networks with trapped entanglements and dangling chains. *Macromolecules* **1989**, *22*, 284−289.
(30) Milner, S. T.; McLeish, T. C. B. Parameter-Free Theory for Stress Relaxation in Star Polymer Melts. *Macromolecules* **1997**, *30* (7), 2159−2166.
(31) Milner, S. T.; McLeish, T. C. B. Reptation and contour-length fluctuations in melts of linear polymers. *Phys. Rev. Lett.* **1998**, *81* (3), 725−728.
(32) McLeish, T. C. B. Tube theory of entangled polymer dynamics. *Adv. Phys.* **2002**, *51* (6), 1379−1527.
(33) Vega, D. A.; Gómez, L. R.; Roth, L. E.; Ressia, J. A.; Villar, M. A.; Vallés, E. M. Arm retraction potential of branched polymers in the absence of dynamic dilution. *Phys. Rev. Lett.* **2005**, *95*, 166002.
(34) Chassé, W.; Lang, M.; Sommer, J.-U.; Saalwächter, K. Correction to cross-link density estimation of PDMS networks with precise consideration of networks defects. *Macromolecules* **2015**, *48*, 1267−1268.
(35) Doi, M.; Kuzuu, N. Y. Rheology of star polymers in concentrated solutions and melts. *J. Polym. Sci., Polym. Lett. Ed.* **1980**, *18* (12), 775−780.
(36) Pearson, D. S.; Helfand, E. Viscoelastic properties of star-shaped polymers. *Macromolecules* **1984**, *17*, 888−895.
(37) Villar, M. A.; Bibbó, M. A.; Vallés, E. M. Influence of pendant chains on mechanical properties of model poly(dimethylsiloxane) networks. 1. analysis of the molecular structure of the network. *Macromolecules* **1996**, *29* (11), 4072−4080.
(38) Macosko, C. W.; Miller, D. R. A new derivation of average molecular weights of nonlinear polymers. *Macromolecules* **1976**, *9* (2), 199−206.
(39) Miller, D. R.; Sarmoria, C. In-out recursive probability modeling of branched step-growth polymerizations. *Polym. Eng. Sci.* **1998**, *38* (4), 535−557.

DOI: 10.1021/acs.macromol.6b02784
Macromolecules 2017, 50, 2964−2972